Toward a Switchable Molecular Rotor. Unexpected Dynamic Behavior of Functionalized Overcrowded Alkenes

Anne Marie Schoevaars,[†] Wim Kruizinga,[†] Robert W. J. Zijlstra,[†] Nora Veldman,[‡] Anthony L. Spek,[‡] and Ben L. Feringa*[,†]

Department of Organic and Molecular Inorganic Chemistry, Groningen Center for Catalysis and Synthesis, University of Groningen, Nijenborgh 4, 9747 AG Groningen, The Netherlands, and Department of Crystal & Structural Chemistry, Bijvoet Center for Biomolecular Research, Utrecht University, Padualaan 8, 3584 CH Utrecht, The Netherlands

Received November 26, 1996[⊗]

In an approach toward a photochemically bistable molecular rotor the synthesis of *cis*-**1a** and *trans*-**1b** isomers of 2-(2,6-dimethylphenyl)-9-(2′,3′-dihydro-1′*H*-naphtho[2,1-*b*]thiopyran-1′-ylidene)-9H-thioxanthene (**1**), being sterically overcrowded alkenes functionalized with an *o*-xylyl group as a rotor, is described. The key steps in the synthesis are a Suzuki coupling to attach the xylyl moiety and a diazo-thioketone coupling with subsequent desulfurization to introduce the central olefinic bond in **1**. The X-ray structure of *cis*-**1a** revealed an anti-folded helical conformation. Dynamic NMR studies on both isomers were performed, to elucidate the kinetics of their rotation processes and to investigate the possibility to control the biaryl rotation by photochemical *cis*-*trans* isomerization. A rotation barrier was found by coalescence spectroscopy for *cis*-**1a**: $\Delta G_c^{\ddagger} = 22 \pm 1$ kcal mol^{-1} in DMSO-d_6. 2D exchange spectroscopy (EXSY) showed barriers for *cis*-**1a**: $\Delta G_{303}^{\ddagger}$ 19.0 ± 0.2 kcal mol^{-1} and *trans*-**1b**: $\Delta G_{303}^{\ddagger} = 19.7 \pm 0.2$ kcal mol^{-1} in DMSO-d_6, respectively. Molecular mechanics and semiempirical calculations support the unexpected higher barrier for *trans*-**1b**. Since the rotation barriers are different for the *cis* and *trans* isomer, it can be concluded that control of a second mechanical effect, e.g. the rate of rotation of an attached biaryl rotor, is feasible in a photochemically switchable system.

Introduction

The development of functional devices at the molecular and supramolecular level has attracted considerable interest during the last decade.[1,2] Elegant examples of functional molecular devices were reported recently, among them a "molecular brake" by Kelly,[3] a "molecular turnstile" by Moore,[4] a "light-switchable catalyst" by Rebek,[5] "photoresponsive crown ethers" by Shinkai,[6] "photoswitchable fluorophores" by Lehn,[7] and "chiroptical molecular switches".[8] Extensive research in our group on sterically overcrowded alkenes provided the basis for the application of these compounds as optical switches to control chirality of molecules and mesoscopic materials.[8] These molecular switches are based on a photochemical *cis*−*trans* isomerization of helically shaped alkenes which simultaneously inverts the helicity of the molecules. Optical data storage[9] is one major objective for such photochromic bistable organic molecules, but photochemical control of other functions in multicomponent devices is an important challenge as well. An example of a gated molecular system based on chiroptical molecular switches in which fluorescence is reversibly modulated was demonstrated recently.[10] Functionalization of the optical switches with a rotor would open the possibility to control a mechanical effect (e.g. the rate of rotation around a single bond) by the photochemical *cis*−*trans* isomerization, due to the difference in steric hindrance in the *cis* and the *trans* isomer. This concept in fact represents the molecular analog of an accelerator in an ordinary machine or a brake, if it is possible to block the rotation completely in one of the isomers at a specific temperature.

In this paper we describe the synthesis of a photochemically bistable molecular rotor and dynamic NMR studies on both isomers, to elucidate the kinetics of their rotation processes and to investigate the feasibility to control this mechanical effect by a chiroptical molecular switch. Although an effective photochemical *cis*−*trans* isomerization could not be achieved in this model system since the UV/vis absorption spectra of the isomers are nearly identical,[11] unexpected dynamic behavior was observed.

Results and Discussion

The principle of a photochemical switchable molecular rotor is shown in Scheme 1. Compound **1**, a thioxanthene-based overcrowded ethylene which can adopt a *cis*-

[†] University of Groningen.
[‡] Utrecht University.
[⊗] Abstract published in *Advance ACS Abstracts,* July 1, 1997.

(1) Feynman, R. P. In *Miniaturization*; Gilbert, H. D., Ed.; Reinhold: New York, 1961; p 282.
(2) (a) Drexler, K. E. *Nanosystems: Molecular Machinery, Manufacturing and Computation*; Wiley: New York, 1992. (b) Lehn, J.-M. *Supramolecular Chemistry*; VCH: Weinheim, 1995.
(3) Kelly, T. R.; Bowyer, M. C.; Bhaskar, K. V.; Bebbington, D.; Garcia, A.; Lang, F.; Kim, M. H.; Jette, M. P. *J. Am. Chem. Soc.* **1994**, *116*, 3657.
(4) Bedard, T. C.; Moore, J. S. *J. Am. Chem. Soc.* **1995**, *117*, 10662.
(5) Würthner, F.; Rebek, J., Jr. *Angew. Chem., Int. Ed. Engl.* **1995**, *34*, 446.
(6) Shinkai, S.; Ogawa, T.; Kusano, Y.; Manabe, O.; Kikukawa, K.; Goto, T.; Matsuda, T. *J. Am. Chem. Soc.* **1982**, *104*, 1960.
(7) Tsivgoulis, G. M.; Lehn, J.-M. *Angew. Chem., Int. Ed. Engl.* **1995**, *34*, 1119.
(8) (a) Feringa, B. L.; Jager, W. F.; de Lange, B.; Meijer, E. W. *J. Am. Chem. Soc.* **1991**, *113*, 5468. (b) Jager, W. F.; de Jong, J. C.; de Lange, B.; Huck, N. P. M.; Meetsma, A.; Feringa, B. L. *Angew. Chem., Int. Ed. Engl.* **1995**, *34*, 348. (c) Feringa, B. L.; Huck, N. P. M.; van Doren, H. A. *J. Am. Chem. Soc.* **1995**, *117*, 9929.
(9) For reviews see: Feringa, B. L.; Jager, W. F.; de Lange, B. *Tetrahedron* **1993**, *49*, 8267. Feringa, B. L.; Huck, N. P. M.; Schoevaars, A. M. *Adv. Mater.* **1996**, *8*, 681.
(10) Huck, N. P. M.; Feringa, B. L. *J. Chem. Soc., Chem. Commun.* **1995**, 1095.
(11) Currently this concept is extended to an effectively switchable system by the attachment of electron-donating and -withdrawing groups in the molecule in order to increase the difference of the UV spectra of the *cis* and the *trans* isomer.[8b]

S0022-3263(96)02210-4 CCC: $14.00

Scheme 1

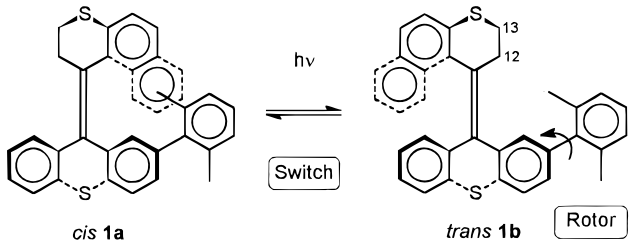

or *trans*-geometry and is extended with a xylyl group as a rotor, was designed as a model system. The presence of the *o*-methyl groups of the rotor are expected to cause restricted rotation around the biaryl bond due to steric interactions with the upper part of the molecule. The influence of these steric effects on the rate of rotation is presumed to be different in the *cis* and the *trans* isomers of **1**. Therefore the rate of rotation might be controlled by a photochemical *cis*−*trans* isomerization. Inspection of molecular models suggested severe steric hindrance for biaryl rotation in the *cis* isomer compared to the *trans* isomer, as a result of interactions with the upper part of the molecule due to the influence of the large naphthalene unit facing the rotor in the first case compared to the small methylene group in the latter. Advantageous are also the singlets in the ^{1}H-NMR spectra arising from the methyl groups of the xylene rotor, allowing dynamic NMR studies of the rotation process.

A successful synthetic route to **1** is shown in Scheme 2. Key steps in the synthetic scheme are the Suzuki coupling[12] to attach the xylyl rotor to the thioxanthone and the coupling of the upper and lower half of the helical alkene using a diazo-thioketone method.[13] Boronic acid derivative **6** was prepared from 2-bromo-1,3-dimethylbenzene **5** via lithiation, quenching with trimethyl borate and subsequent hydrolysis of the boronic ester. 2-Nitrothioxanthone (**2**)[14] was reduced to the corresponding amine **3**[15] followed by conversion into iodide **4** via a diazotization procedure. Boronic acid **6** was connected to the thioxanthone via a palladium-catalyzed coupling[16] to provide the xylyl-substituted thioxanthone **7**. All reactions proceed in good yields. Reaction of ketone **7** with P_2S_5 in toluene resulted in thioketone **8** in 82% yield, which was reacted with hydrazone **9** in a diazo-thioketone coupling[13] to provide episulfide **10** as a *cis*−*trans* mixture. Desulfurization of the episulfide with copper−bronze in *p*-xylene under reflux conditions failed, and the use of $LiAlH_4$ in refluxing toluene/ether was not successful either. Finally we were able to desulfurize **10** using PPh_3 in boiling toluene.[17] The desired alkene **1** was obtained as a *cis*−*trans* mixture with a *cis*:*trans* ratio of 1.3:1. The geometrical isomers and the enantiomers (with opposite helicities) of the *cis* as well as the *trans* forms of **1** were readily separated by HPLC using a chiral stationary phase (see Experimental Section).

The crystal structure of *cis*-**1a** is shown in Figure 1. The arrangement about the central double bond is nearly planar (dihedral angles $C_{12}-C_{11}-C_{14}-C_{26}$ = 7.1(11)°; $C_{10}-C_{11}-C_{14}-C_{15}$ = 4.7(11)°). The bond length obtained for the central double bond (1.345(12) Å, $C_{11}-C_{14}$) is a characteristic value for a simple nonconjugated double bond (1.337 Å).[18] The anti-folded helical structure in which the top and bottom halves are tilted down and upward, respectively, relative to the plane of the central double bond, and by which severe nonbonding interactions are avoided, is clearly shown. Both heterocyclic rings in *cis*-**1a** adopt twisted-boat conformations relieving the steric interactions present in this molecule. In the crystal structure the xylyl moiety is rotated strongly out of the plane of the adjacent aryl group resulting in a torsion angle of this biaryl unit of −86.6(10)° ($C_{18}-C_{17}-C_{27}-C_{32}$).

In the ^{1}H-NMR spectra the isomers can be distinguished on the basis of the resonance of the methyl groups of the xylyl moiety. Furthermore, both isomers *cis*-**1a** and *trans*-**1b** show two separate methyl signals in their ^{1}H-NMR spectra at 30 °C, indicating slow biaryl rotation on the NMR time scale. The chemical shifts of the methyl groups in DMSO-d_6 are 0.64 and 1.62 ppm for *cis*-**1a** and 1.91 and 2.18 ppm for *trans*-**1b**, respectively. The large chemical shift difference between the methyl signals of *cis*-**1a** can be explained by the difference in electronic environment of both groups. From the X-ray structure of *cis*-**1a** (Figure 1) and molecular modeling studies, it becomes evident that one methyl group is pointing toward the aromic upper part of the alkene, while the other methyl is not influenced by this naphthalene moiety. The rotation barriers for *cis*-**1a** and *trans*-**1b** were examined first using temperature dependent ^{1}H-NMR,[19] focussing on the coalescence behavior of the methyl signals. From the difference in chemical shifts of the two methyl absorptions at both sites ($\Delta\nu$) plotted against the temperature, the rate constant (k_c) for rotation at the coalescence temperature can be determined by means of the formula $k_c = 2^{-1/2}\pi\Delta\nu_c$. Substitution of k_c in the Eyring equation gives the free energy of activation for the rotation, i.e. the rotation barrier $\Delta G_c^{\ddagger}$.

A series of ^{1}H-NMR spectra were recorded in the temperature range 313 to 443 K with increments of 10 K. The measurements were carried out for both isomers simultaneously to ensure exact identical conditions using a mixture of *cis*-**1a** and *trans*-**1b** in DMSO-d_6. The results are presented in Figure 2. For the *cis* isomer $\Delta\nu$ decreases with increasing temperature but not to complete coalescence.

Extrapolation of the graph, however, resulted in an estimated coalescence temperature of 473 ± 5 K and a rotation barrier $\Delta G_c^{\ddagger}$ of 22 ± 2 kcal mol^{-1}. Much to our surprise, for the *trans* isomer we did not observe a significant change in $\Delta\nu$ in the temperature range studied; therefore, no estimation of the coalescence temperature could be made. Although a lower rotation barrier of the *trans* isomer was expected, these experiments show that the barrier of the *trans* isomer is even higher than that of the *cis* isomer.

(12) Miyaura, N.; Yanagi, T.; Suzuki, A. *Synth. Commun.* **1981**, *11*, 513.

(13) (a) Barton, B. H. R.; Willis, B. J. *J. Chem. Soc., Perkin Trans 1* **1972**, 305. (b) Kellogg, R. M.; Buter, J.; Wassenaar, S. *J. Org. Chem.* **1972**, *37*, 4045. (c) Schönberg, A.; König, B.; Singer, E. *Chem. Ber.* **1967**, *100*, 767.

(14) Amstutz, E. D.; Neumoyer, C. R. *J. Am. Chem. Soc.* **1947**, *69*, 1922.

(15) Mann, F. G.; Turnbull, H. J. *J. Chem. Soc.* **1951**, 747.

(16) Yang, Y. *Synth. Commun.* **1989**, *19*, 1001. Procedure as described in this reference, except that 1.5 equiv of $Ba(OH)_2$ was used instead of 3 equiv of $NaHCO_3$.

(17) Seitz, G.; Hoffmann, H. *Synthesis* **1977**, 201.

(18) *Handbook of Chemistry and Physics*; Astle, M. J., Weast, R. C., Eds.; CRC Press: Boca Raton, FL, 1980; F-218.

(19) (a) Oki, M. *Applications of Dynamic NMR Spectroscopy to Organic Chemistry*. In *Methods of Stereochemical Analysis*; Marchand, A. P., Ed.; VCH: Weinheim, 1985; Vol. 4. (b) Sandström, J. *Dynamic NMR Spectroscopy*; Academic Press: New York, 1982. (c) Binsch, G.; Kessler, H. *Angew. Chem., Int. Ed. Engl.* **1980**, *19*, 411.

Scheme 2

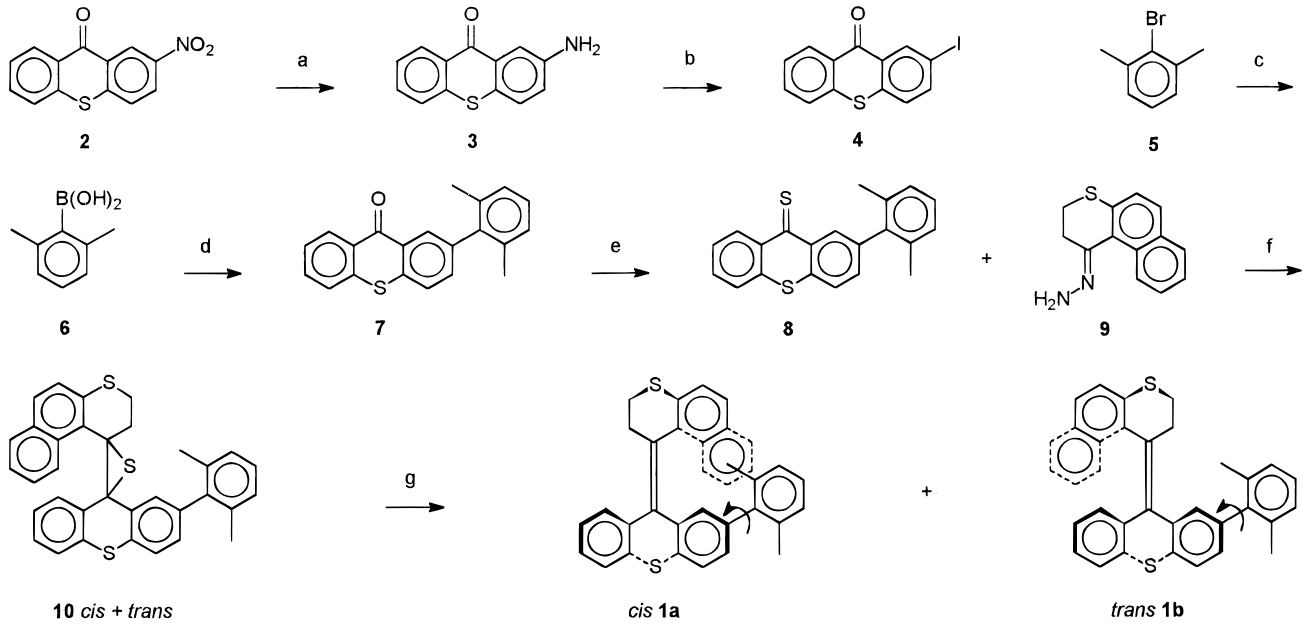

a) $SnCl_2$, HCl, AcOH, 74%. b) 1. $NaNO_2$, HCl, 0-5°C, 2. KI, 62%. c) 1. sec-BuLi, 2. $B(OMe)_3$, 3. HCl, 51%. d) $Pd(PPh_3)_4$, $Ba(OH)_2$ (aq), DME, 82%. e) P_2S_5, toluene, 82%. f) Ag_2O, $MgSO_4$, KOH/MeOH, CH_2Cl_2, -20°C, 82%. g) PPh_3, toluene, 55%.

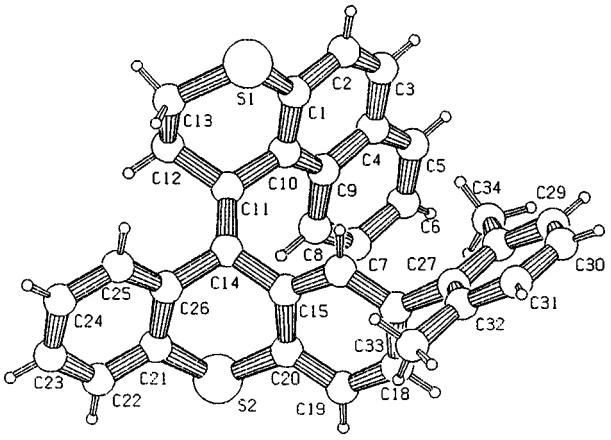

Figure 1. PLUTON diagram of the X-ray structure of *cis*-**1a** with adopted numbering scheme.

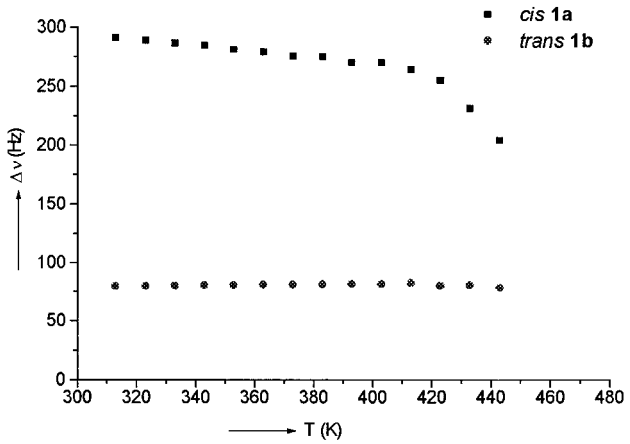

Figure 2. Difference in chemical shifts of the two methyl absorptions ($\Delta\nu$) of **1a** and **1b** in DMSO-d_6 as a function of the temperature.

Since quantitative comparison of the rotation barriers was not possible using coalescence studies, we studied the rotation process by 2D EXSY spectroscopy, a powerful technique for determining exchange rate constants (and via the Eyring equation free energies of activation) in the region of slow exchange on NMR time scale.[20]

As the dynamic behavior of the xylene rotor, within either *cis*-**1a** or *trans*-**1b**, resembles the situation of a two-site exchange system (of two methyl groups on a xylyl substituent) with equal populations and spin-lattice relaxation times within each others error margins, the exchange rate (= rotation rate) k can be calculated directly from the ratio of cross- and auto-peak integrations (a_{AA}/a_{AB}) and the mixing time (t_m), using the formula $(a_{AA}/a_{AB}) = (1 - kt_m)/kt_m$.[20c] The experiments were carried out using a mixture of *cis* and *trans* isomers of **1** in DMSO-d_6 at temperatures from 303 to 363 K. The results are presented in Figure 3.

As expected, a linear relationship was found for the rotation barrier as a function of the temperature. Via an Eyring plot ($\ln[kh/k_BT]$ plotted against $1/T$), the values for the enthalpies and entropies of activation were calculated and presented together with the rotation barriers at 303 K in Table 1. The estimated rotation barrier (at T_c) of *cis*-**1a** in DMSO-d_6 from the coalescence studies ($\Delta G_{473}^{\ddagger}$) of 22 ± 1 kcal mol^{-1} is indeed in the same order of magnitude compared to the results for *cis*-**1a** from the exchange spectroscopy in DMSO-d_6 in which $\Delta G_{473}^{\ddagger}$ = 23.6 ± 0.2 kcal mol^{-1} (calculated from $\Delta H^{\ddagger}$ and $\Delta S^{\ddagger}$). In accordance with the results of the coalescence studies the barrier of *trans*-**1b** is higher than that of *cis*-**1a** at ambient temperature. At 303 K a small but significant difference of 0.7 kcal mol^{-1} in rotation barriers for the *cis* and *trans* isomers was determined.

For a better understanding of the unexpected higher rotation barrier of *trans*-**1b**, we have employed both

(20) (a) Jeener, J.; Meier, B. H.; Bachmann, P.; Ernst, R. R. *J. Chem. Phys.* **1979**, *71*, 4546. (b) Macura, S.; Ernst, R. R. *Mol. Phys.* **1980**, *41*, 95. (c) Bodenhausen, G.; Ernst, R. R. *J. Am. Chem. Soc.* **1982**, *104*, 1304.

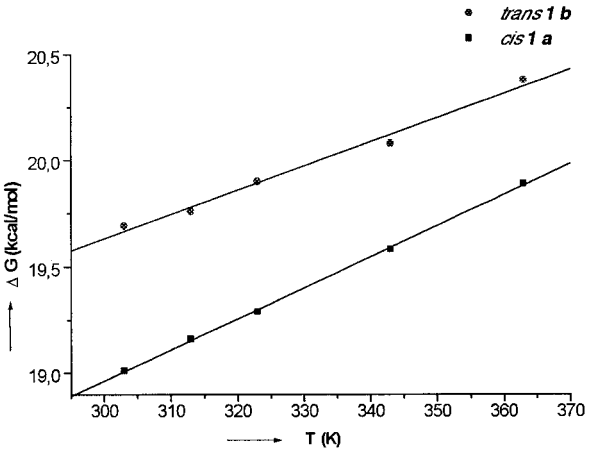

Figure 3. Rotation barriers ($\Delta G^{\ddagger}$) of the biaryl rotation in *cis*-**1a** and *trans*-**1b** based on the EXSY experiments in DMSO-d_6.

Table 1. Kinetic Data Exchange Spectroscopy

compound	$\Delta H^{\ddagger}$ (kcal/mol)	$\Delta S^{\ddagger}$ (cal/mol K)	$\Delta G_{303}^{\ddagger}$ (kcal/mol)
cis-**1a**	14.3	−15.5	19.0 ± 0.2
trans-**1b**	16.2	−11.4	19.7 ± 0.2

molecular mechanics calculations using the TRIPOS[21] force field as implemented in SYBYL and semiempirical AM1[22] calculations with MOPAC93.[23] It should be noted that especially in the case of the AM1 calculations caution has to be taken in defining the reaction path. Since AM1 takes each last optimized coordinate as a starting point for the next step, biased reaction paths are likely to occur. It is therefore necessary to investigate the reaction path over a 360° range, although C_2-symmetry is present in the xylyl rotor. In fact conformations in the vicinity of maximum rotational energy are recognized by significant distortions leading to symmetry breaking in this part of the molecule, which implies that the total reaction path of the rotation has to be investigated.

The structure of the AM1 optimized lowest energy conformation of *cis*-**1a** (Figure 4) is in agreement with the X-ray structure (Figure 1); the twisted boat conformations of the heterocyclic rings are confirmed in the calculated structure. Only a minor difference is found in the torsion angles of the biaryl units, −86.6(10)° in the X-ray structure ($C_{18}-C_{17}-C_{27}-C_{32}$) versus 90° in the calculated lowest energy conformation. This difference might be explained by crystal packing effects.

The results of the computational calculations are presented in Table 2. Both the molecular mechanics and semiempirical results show the same trend. In the case of *trans*-**1b** an increase of the rotation energy barrier of 1.2 kcal mol^{-1} (AM1) to 1.7 kcal mol^{-1} (TRIPOS) in comparison with *cis*-**1a** is predicted.

Analysis of the AM1 transition state (TS) structures for the biaryl rotations provides a satisfactory explanation for the surprisingly higher barrier of rotation in, what we expected to be the less sterically hindered, *trans*-**1b**. As can be seen in Figure 5, in the *trans*-**1b** transition

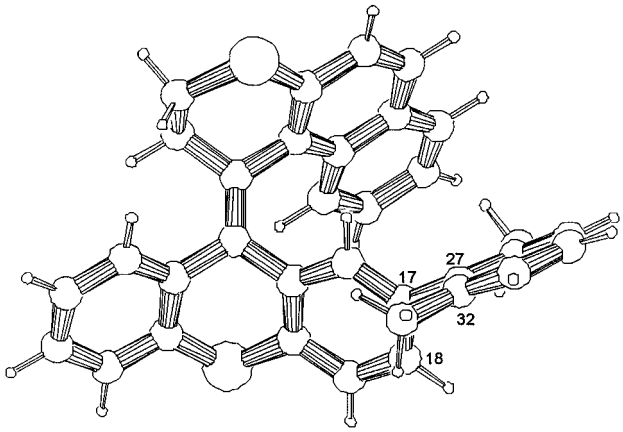

Figure 4. AM1-optimized lowest energy conformation of *cis*-**1a**.

Table 2. Calculated Minimal Energies and Rotation Barriers of *cis*-1a and *trans*-1b

	TRIPOS		AM1	
	E_{min} (kcal/mol)	ΔE_{rot} (kcal/mol)	E_{min} (kcal/mol)	ΔE_{rot} (kcal/mol)
cis-**1a**	15.7	17.0	138.0	16.6
trans-**1b**	15.7	18.7	137.3	17.8

state (TS) the methyl group (C_{34}) of the *o*-xylyl rotor gets entangled between the two hydrogens at C_{13}. The distance between the methyl and the ring hydrogens is 2.1 Å, which is well inside their van der Waals radii and is indicative of a significant repulsive interaction between the two halves of the molecule.

Examination of the *cis*-**1a** TS structure (Figure 5) does not lead to the discovery of such intimate contacts, although one of the *o*-xylyl methyl groups is pointing toward the naphthyl moiety in the upper part of the molecule. Typical distances between the methyl hydrogens and naphthyl carbon atoms are 3.0 Å. Careful analysis of the geometry of this TS structure confirms this interaction to be the sterically demanding one. The relatively large naphthalene unit in the upper part of the molecule, which causes the hindrance in the *cis* isomer, bends away from the central part of the molecule as is also clearly seen in the X-ray structure (Figure 1), leaving enough space for faster rotation of the xylyl unit in *cis*-**1a** compared to *trans*-**1b**. Furthermore the $C_{19}-C_{18}-C_{17}-C_{27}$ dihedral angle shifts from 180.0° in the lowest energy conformation to 162.3° in the TS structure (Figure 5). In other words, the *o*-xylyl group appears to bend away from the naphthyl, thus reducing the steric interactions between its methyl groups and the opposite naphthyl moiety in the other half of the molecule.

From the values of $\Delta H^{\ddagger}$ and $\Delta S^{\ddagger}$ (Table 1) it can be seen that the higher rotation barrier of *trans*-**1b** is caused by a higher $\Delta H^{\ddagger}$. The different nature of the interactions in the transition states for the biaryl rotation in *cis*-**1a** and *trans*-**1b** also provides a reasonable explanation for the inverse trend in the observed $\Delta S^{\ddagger}$ of rotation (Table 1). Although the contacts in the case of *trans*-**1b** are more pronounced and thus leading to a higher $\Delta H^{\ddagger}$, a relatively small region of the molecule (the ethylene bridge $C_{12}-C_{13}$) is involved in the interaction with the *o*-xylyl rotor. In the case of *cis*-**1a**, however, the much larger naphthyl moiety is involved in the interaction with the rotor, thus restricting the conformational freedom in a significantly larger part of the molecule in the TS. The confinement of the larger part of the molecule in the

(21) (a) Lowe, J. P. *Barriers to Internal Rotation about single bonds* in *Progress in Physical Organic Chemistry*; Wiley: New York, 1968; Vol. 6, p 1. (b) Dixon, D. A.; Zeroka, D.; Wendoloski, J. J.; Wasserman, Z. R. *J. Phys. Chem.* **1985**, *89*, 5334.

(22) (a) Dewar, M. J. S.; Zoebisch, E. G.; Healy, E. F.; Stewart, J. J. P. *J. Am. Chem. Soc.* **1985**, *107*, 3902. (b) Dewar, M. J. S.; Yuan, Y.-C. *Inorg. Chem.* **1990**, *29*, 3881.

(23) Stewart, J. J. P. *Quant. Chem. Prog. Exch.* **1990**, *10*, 86.

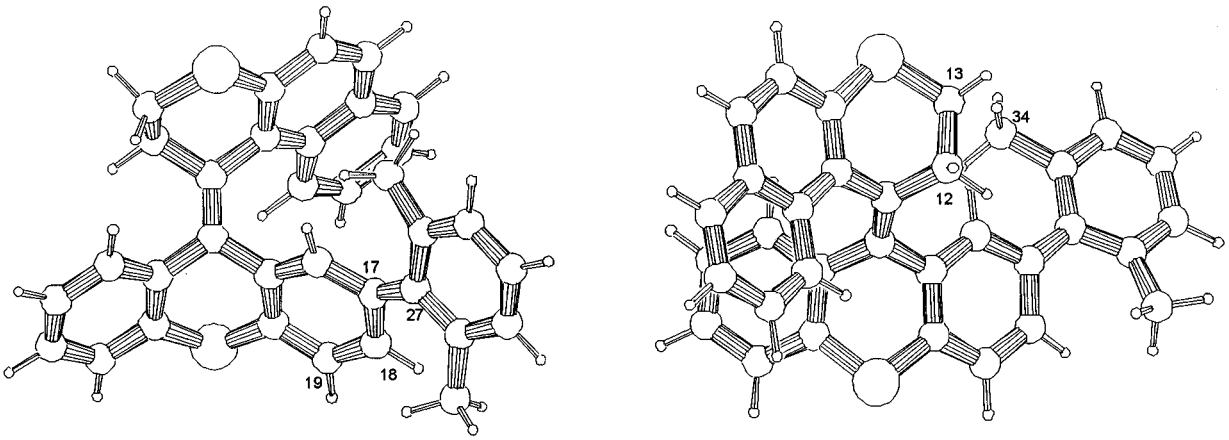

Figure 5. AM1-optimized *cis*-**1a** (left) and *trans*-**1b** transition state structures for biaryl rotation.

latter case should lead to a larger $\Delta S^{\ddagger}$ of rotation, which is in agreement with the experimental findings.

In summary, the assumption that *cis*-alkenes are the sterically more hindered structures when compared with their *trans* counterparts does not seem to hold for such helically shaped overcrowded alkenes. As can be seen in Figure 1, the considerable pitch of these helical structures introduces a large separation between upper and lower halve of the alkene in its *cis* configuration, especially in the regions remote from the central olefinic bond. This leads to more conformational freedom then expected on the basis of a *cis*-alkene geometry.

On the basis of these results and the additional observation of unexpected dynamical behavior in several other helicenes with related structural features,[24] it is suggested that the "classical picture" regarding steric hindrance in *cis* and *trans* isomers is at least incomplete for such helically shaped inherently dissymetric alkenes.

Conclusions

It can be concluded that control of a second mechanical effect, the rate of rotation of a rotor, by *cis*−*trans* isomerization of a sterically overcrowded alkene is feasible, since the rates of rotation are different for the *cis* and *trans* isomer. In contrast with expectation the rotation barrier of the *trans* isomer proved to be higher than that of the *cis* isomer. Modifications to increase the difference in UV/vis absorptions and to enhance the difference in rotation barriers between the *cis* and the *trans* isomer are necessary to achieve an effective photochemically switchable system. Such studies are currently in progress.

Experimental Section

General Remarks. Melting points are uncorrected. ^{1}H NMR data were recorded on a Varian Gemini 200, a Varian VXR 300, or a Varian Unity 500 (at 200, 300, or 500 MHz, respectively). ^{13}C NMR data were recorded on a Varian Gemini 200 or a Varian VXR 300 (at 50.32 or 75.48 MHz, respectively). All shifts are denoted relative to the solvent used. Merck silica gel 60 (230−400 mesh ASTM) was used for chromatography. Solvents were purified using standard procedures. 2-Bromo-1,3-dimethylbenzene (**5**) was purchased from Across Chimica and used without purification. All other reagents are commercially available and were used without purification.

Exchange Spectroscopy Experiments. The EXSY spectra were recorded at 300 MHz on a Varian VXR 300 with the NOESYPH pulse sequence supplied by the Varian software. For phase cycling, the States−Haberkorn method[25] was used; each of the 512 increments was the accumulation of 16 scans. The relaxation delay was 1.5 s. The measurements were carried out at each temperature with several mixing times (0.025−1.5 s) to ensure an appropriate choice of the mixing time. Before Fourier transformation, the FID's were multiplied by $p/2$ shifted sine-bell function in the F_2 domain and in the F_1 domain. The data file was zero-filled, resulting in a spectrum of 1K × 1K real data points. A base-plane correction was applied to the 2D spectrum. Peak volumes were determined by integration of the peaks of interest.

Computational Details. In all rotation barrier calculations, the geometry of the whole molecule was optimized as a function of the rotation around the *o*-xylyl C−C bond. The rotational energy barriers were obtained by 5° increments on the dihedral angle defined. In the case of the AM1 calculations, the step size was reduced to 1° increments in the regime of the potential energy barrier maximum. TRIPOS force field calculations were performed within SYBYL on a SG Indy. BFGS gradient minimization with convergence criterion of 0.001 cal/mol Å was applied. AM1 calculations were performed within MOPAC93 on a HP Apollo. For the AM1 geometry (and reaction path) optimizations, the BFGS converger was used together with the tightest possible convergence criterion of the SCF energy (keyword GNORM = 0). For strained structures at reaction coordinates in the vicinity of the rotational barrier maximum, Pulay's converger was used to improve the convergence of the SCF procedure.

Crystal Data for *cis*-1a. $C_{34}H_{26}S_2$, monoclinic, space group $P2_1/c$, a = 12.9026(10), b = 14.8056(15), c = 18.0919(15) Å, β = 133.733(10), V = 2497.3(6) Å^3, Z = 4, d_x = 1.327 g cm^{-3}. X-ray data for a colorless, plate-shaped crystal cut to size (0.05 × 0.38 × 0.38 mm) were collected on an ENRAF-NONIUS CAD4T on rotating anode [Mo Kα, graphite monochromated, λ = 0.71073 Å, Θ_{max} = 25°, ω-scan, T = 150 K]. The structure was solved by direct methods (SHELXS86) and refined on F^2 (SHELXL-93). Hydrogen atoms were taken into account at calculated positions. Final R_1 value 0.0829 [2018 reflections with $I > 2\sigma(I)$], wR_2 = 0.1565 [4376 reflections], S = 1.018, 327 parameters. Atomic coordinates, bond lengths and angles, and thermal parameters have been deposited at the Cambridge Crystallographic Data Centre and can be obtained, on request, from the Director, Cambridge Crystallographic Data Centre, 12 Union Road, Cambridge, CB2 1EZ, UK.

(2,6-Dimethylphenyl)boronic Acid (6). A stirred solution of 1.00 g (5.41 mmol) of 2-bromo-1,3-dimethylbenzene (**5**) in 50 mL of THF was cooled to −78 °C under a nitrogen atmosphere, 5.94 mmol of *sec*-BuLi (4.57 mL of 1.3 M solution in hexane) was added via a syringe, and the temperature of the mixture was maintained at −78 °C for 1 h. The temperature was gradually raised to −50 °C, and 0.62 mL (5.41 mmol)

(24) Harada, N.; Saito, A.; Koumura, N.; Roe, C. D.; Jager, W. F.; Zijlstra, R. W. J.; de Lange, B.; Feringa, B. L. *J. Am. Chem. Soc.*, submitted for publication.

(25) States, D. J.; Haberkorn, R. A.; Ruben, D. J. *J. Magn. Reson.* **1982**, *48*, 286.

of $B(OMe)_3$ was added. The mixture was warmed to room temperature, and 200 mL of ether was added. The organic layer was washed with 5% HCl solution (100 mL) and water (100 mL) and dried over $MgSO_4$. Evaporation of the solvents gave the crude product which was crystallized from ether and hexanes to give **6** as white needles (0.41 g, 2.73 mmol, 51%): mp = 121 °C; ^{1}H NMR (acetone d_6): δ 2.31 (s, 6H), 6.90 (d, J = 7.3 Hz, 2H), 7.04 (t, J = 7.3 Hz, 1H), 7.20 (s, 2H); ^{13}C NMR (acetone-d_6): δ 36.13, 140.38, 142.25, 153.46, 220.10; HRMS calcd 150.085, found 150.085.

2-Aminothioxanthen-9-one (3). This compound was prepared from 2-nitro-9*H*-thioxanthen-9-one **2** (2.00 g, 7.78 mmol) following the procedure described by Mann and Turnbull.[15] Amine **3** was obtained as a yellow powder (1.30 g, 5.73 mmol, 74%): mp = 227−228 °C ^{1}H NMR ($CDCl_3$): δ 3.95 (bs, 2H), 7.06 (dd, J = 8.6, 3.0 Hz, 1H), 7.42 (d, J = 8.5 Hz, 1H), 7.46−7.61 (m, 3H), 7.92 (d, J = 3.0 Hz), 8.63 (dd, J = 6.9, 0.9 Hz); HRMS calcd 227.040, found 227.040.

2-Iodothioxanthen-9-one (4). A suspension of amine **3** (0.55 g, 2.42 mmol), 1.2 mL concentrated HCl, and 1 g of ice was stirred and cooled with an ice bath. An ice-cooled solution of $NaNO_2$ (0.19 g, 2.78 mmol) in 1 mL of water was added dropwise, the temperature being kept at 0−5 °C. After stirring the suspension for 15 min, it was slowly poured into a solution of 1.43 g (8.61 mmol) of KI in 5 mL of water. The mixture was warmed till the evolution of gas ceased and allowed to cool to room temperature. CH_2Cl_2 (100 mL) was added, and the organic layer was separated, washed successively with 10% aqueous NaOH, water, and 5% aqueous $NaHSO_3$, and then dried over $MgSO_4$. Purification of the crude product by column chromatography (silica gel, CH_2Cl_2) afforded **4** as a yellow solid (0.51 g, 1.51 mmol, 62%): mp = 147.6 °C; ^{1}H NMR ($CDCl_3$): δ 7.31 (dd, J = 7.3, 2.6 Hz, 1H), 7.47−7.71 (m, 3H), 7.88 (dd, J = 8.6, 2.1 Hz, 1H), 8.60 (d, J = 8.1 Hz, 1H), 8.93 (d, J = 1.7 Hz, 1H); ^{13}C NMR ($CDCl_3$): δ 90.76, 126.04, 126.52, 127.42, 128.40, 129.89, 130.40, 132.50, 136.73, 138.49, 140.55, 178.20; HRMS calcd 337.926, found 337.926.

2-(2,6-Dimethylphenyl)thioxanthen-9-one (7). A mixture of **4** (1.00 g, 2.96 mmol), $Pd(PPh_3)_4$ (0.09 g, 0.08 mmol), and DME (20 mL) was stirred under a nitrogen atmosphere for 10 min. Boronic acid **6** (0.49 g, 3.26 mmol) and a suspension of 1.54 g (4.90 mmol) of $Ba(OH)_2{\cdot}8H_2O$ in 20 mL of water were subsequently added. The mixture was stirred and refluxed for 18 h and allowed to cool to room temperature. Ether (100 mL) was added, and the water layer was separated and extracted with ether (50 mL) and dichloromethane (50 mL). The combined organic layers were dried over $MgSO_4$, and the solvents were evaporated. Purification of the crude product by column chromatography (silica gel, CH_2Cl_2/hexanes, 1/1) afforded **7** as a yellow solid (0.77 g, 2.44 mmol, 82%): mp = 163.1 °C; ^{1}H NMR ($CDCl_3$): δ 2.05 (s, 6H), 7.12−7.20 (m, 3H), 7.43−7.49 (m, 2H), 7.62−7.68 (m, 3H), 8.45 (d, J = 1.8 Hz, 1H), 8.64 (d, J = 8.1 Hz); ^{13}C NMR ($CDCl_3$): δ 20.70, 125.91, 126.11, 126.19, 127.37, 127.44, 129.16, 129.22, 129.79, 130.07, 132.15, 133.39, 135.51, 135.89, 137.14, 139.28, 140.06, 179.92; HRMS calcd 316.092, found 316.092.

2-(2,6-Dimethylphenyl)thioxanthene-9-thione (8). A solution of **7** (0.72 g, 2.28 mmol) in 25 mL of toluene was stirred under a nitrogen atmosphere whereupon P_2S_5 (1.01 g, 4.56 mmol) was added, and the mixture was subsequently heated at reflux. After 10 min the dark green mixture was filtered hot, the residue was washed with toluene and CH_2Cl_2 till the filtrate was slightly green, and the solvents were evaporated. Purification of the crude product by column chromatography (silica gel, CH_2Cl_2) and crystallization from ethanol afforded **8** as dark green crystals (0.62 g, 1.87 mmol, 82%): mp = 100.8 °C; ^{1}H NMR ($CDCl_3$): δ 2.08 (s, 6H), 7.13−7.18 (m, 3H), 7.43−7.46 (m, 2H), 7.60−7.67 (m, 3H), 8.86 (d, J = 1.46 Hz, 1H), 9.00 (d, J = 8.42 Hz, 1H); ^{13}C NMR ($CDCl_3$): δ 20.82, 125.86, 125.98, 126.85, 127.44, 130.14, 131.49, 131.75, 132.80, 133.21, 133.61, 135.93, 137.58, 137.62, 139.76, 140.07, 211.07; HRMS calcd 332.069, found 332.069.

***cis*- and *trans*-Dispiro[2,3-dihydro-1*H*-naphtho[2,1-*b*]thiopyran-1,2′-thiirane-3′,9″-[2″-(2,6-dimethylphenyl)-9″*H*-thioxanthene]] (10).** A stirred solution of hydrazone **9** (340 mg, 1.52 mmol) in anhydrous CH_2Cl_2 (30 mL) was cooled to −5 °C, whereupon $MgSO_4$ (approximately 0.5 g), Ag_2O (0.6 g, 2.6 mmol), and a saturated solution of KOH in MeOH (0.3 mL) were successively added. After 15 min, the mixture turned deep red, and after another 30 min of stirring at −5 °C, the solution was filtered into another ice-cooled flask, and the remaining residue was washed with cold CH_2Cl_2 (15 mL). To this clear solution was added thioketone **8** in small portions. Evolution of nitrogen was observed, and the deep red color disappeared. The thioketone was added until the evolution of nitrogen had ceased; a total of 360 mg (1.08 mmol) was necessary. After stirring for 3 h at room temperature, the solvents were evaporated. Purification of the crude product by column chromatography (silica gel, CH_2Cl_2 and subsequently CH_2Cl_2/hexanes, 1/1) and crystallization from ethanol and CH_2Cl_2 afforded **10** as white crystals (0.47 g, 0.89 mmol, 82% based on the thioketone): mp_{cis} = 200.8 °C; ^{1}H NMR ($CDCl_3$, *cis* isomer): δ 0.89 (s, 3H), 1.75 (s, 3H), 2.19−2.27 (m, 1H), 2.49−2.69 (m, 3H), 6.63 (dd, J = 7.8, 1.8 Hz, 1H), 6.80 (d, J = 7.3 Hz, 1H), 6.92 (d, J = 6.4 Hz, 1H), 6.99 (d, J = 7.3 Hz, 1H), 7.05 (d, 1H), 7.11−7.55 (m, 16 H), 7.60 (d, J = 8.4 Hz, 1H), 8.13 (dd, J = 5.9, 3.6 Hz, 1H), 9.10 (d, J = 8.54 Hz, 1H), methyl signals of the *trans* isomer: δ 2.11(s) and 2.19(s); ^{13}C NMR ($CDCl_3$, mixture of *cis* and *trans* isomers): δ 19.78, 20.66, 26.36, 26.76, 36.61, 37.21, 57.90, 58.60, 59.80, 60.50, 122.67, 123.16, 124.01, 124.14, 124.38, 124.49, 125.05, 125.15, 125.51, 125.59, 125.72, 125.83, 125.98, 126.20, 126.51, 126.62, 127.19, 127.21, 127.31, 127.41, 127.49, 127.55, 127.70, 127.73, 127.80, 128.12, 128.20, 128.51, 128.71, 129.69, 130.34, 131.02, 131.16, 131.48, 131.64, 131.91, 132.33, 133.04, 135.69, 135.80, 135.84, 136.26, 136.61, 137.48, 138.17, 138.55, 140.37, 140.97. Anal. Calcd for $C_{34}H_{26}S_3$: C 76.94, H 4.94, S 18.12. Found: C 76.53, H 5.11, S 18.07; HRMS calcd 530.120, found 530.120.

***cis*- and *trans*-2-(2,6-Dimethylphenyl)-9-(2′,3′-dihydro-1′*H*-naphtho[2,1-*b*]thiopyran-1′-ylidene)-9*H*-thioxanthene (1a, 1b).** A mixture of 0.20 g (0.38 mmol, mixture of *cis* and *trans* isomers) of episulfide **10**, 0.12 g (0.46 mmol) PPh_3, and 20 mL of dry toluene was stirred and refluxed for 18 h and then cooled to room temperature. The solvent was evaporated, and the crude product was purified by column chromatography (silica gel, toluene) to give alkene **1** as a *cis*/*trans* mixture in a 1/1 ratio (0.10 g, 0.21 mmol, 55%). Crystallization from ethanol/CH_2Cl_2 afforded crystals of *cis*-**1a** suitable for X-ray analysis (see Supporting Information). Resolution of the enantiomers of the *cis* and *trans* isomers was performed with chiral HPLC employing a (+)-poly(triphenylmethyl methacrylate) column (OT^+) using hexanes/2-propanol 9/1 as eluent (flow 1 mL/min) retention times: $t_{cisI} = t_{transI}$ = 7.9 min, $t_{transII}$ = 10.5 min, t_{cisII} = 13.4 min; mp_{cis} = 236.7 °C; ^{1}H NMR ($CDCl_3$, the data for *cis*-**1a** and *trans*-**1b** in a 2.75/1.00 ratio are given): δ 0.71 (s, 2.20H), 1.72 (s, 2.20H), 1.98 (s, 0.80H), 2.11−2.16 (m, 1H), 2.23 (s, 0.80H), 3.38−3.70 (m, 3H), 6.47 (d, J = 2.0 Hz, 0.73H), 6.48 (m, 0.27H), 6.53 (d, J = 7.8 Hz, 0.27H), 6.59 (dd, J = 7.8, 2.0 Hz, 0.73H), 6.80 (d, J = 7.8 Hz, 0.73H), 6.82 (m, 0.27H), 6.89 (d, J = 7.3 Hz, 0.73 H), 6.98 (t, J = 7.6 Hz, 0.73H), 7.03 (t, J = 7.8 Hz, 0.27H), 7.09−7.23 (m, 2.54H), 7.30−7.44 (m, 3.73H), 7.55−7.63 (m, 3H), 7.66−7.70 (m, 1H), 7.79 (d, J = 8.3 Hz, 0.73 H); ^{13}C NMR ($CDCl_3$, the data for *cis*-**1a** are given): δ 19.73, 20.09, 29.60, 30.02, 124.49, 124.60, 125.83, 126.11, 126.49, 126.65, 126.71, 126.78, 126.86, 127.42, 127.86, 127.92, 127.81, 129.11, 131.95, 132.43, 132.44, 133.99, 134.10, 134.40, 135.90, 136.22, 138.62, 139.00, 140.07; HRMS calcd 498.148, found 498.148.

Supporting Information Available: ^{1}H and ^{13}C NMR spectra of compounds **1**, **4**, **6**, **7**, and **8**; data of coalescence studies and EXSY studies (12 pages). This material is contained in libraries on microfiche, immediately follows this article in the microfilm version of the journal, and can be ordered from the ACS; see any current masthead page for ordering information.

Acknowledgment. Financial support was provided by the Netherlands Organization for Scientific Research (NWO/SON) and Stichting Technische Wetenschappen (STW).

JO962210T